NUCL SCI TECH (2017) 28:52
DOI 10.1007/s41365-017-0204-0

Analog rise-time discriminator for CdZnTe detector

Chuan-Hao Hu[1] · Guo-Qiang Zeng[1] · Liang-Quan Ge[1] · Shi-Long Wei[1] · Jian Yang[1] · Qiang Li[1] · Hong-Zhi Li[2]

Received: 6 April 2016 / Revised: 24 May 2016 / Accepted: 3 June 2016 / Published online: 1 March 2017

Abstract Due to variable time for charge collection, energy resolution of nuclear detectors declines, especially compound semiconductor detectors like cadmium zinc telluride (CdZnTe) detector. To solve this problem, an analog rise-time discriminator based on charge comparison principle is designed. The reference charge signal after attenuation is compared with the deconvoluted and delayed current signal. It is found that the amplitude of delayed current signal is higher than that of the reference charge signal when rise time of the input signal is shorter than the discrimination time, thus generating gating signal and triggering DMCA (digital multi-channel analyzer) to receive the total integral charge signal. When rise time of the input signal is longer than discrimination time, DMCA remains inactivated and the corresponding total integral charge signal is abandoned. Test results show that combination of the designed rise-time discriminator and DMCA can reduce hole tailing of CdZnTe detector significantly. Energy resolution of the system is 0.98%@662 keV, and it is still excellent under high counting rates.

Keywords Analog rise-time discriminator · CdZnTe detector · Charge comparison principle

This work was supported by the Natural Science Foundation of China (NSFC) (No. 41474159), National High-tech R&D Program of China (863 Program) (Nos. 2012AA061803 and 2014AA093403) and Open Foundation of Applied Nuclear Techniques in Geosciences Key Laboratory of Sichuan Province (No. gnzds2014006).

✉ Guo-Qiang Zeng
zgq@cdut.edu.cn

1 Chengdu University of Technology, Chengdu 610059, China

2 National Ocean Technology Center, Tianjin 300112, China

1 Introduction

A cadmium zinc telluride (CdZnTe) detector is characterized by its high atomic number, large width of forbidden band, high detection efficiency and energy resolution at room temperature [1–3]. Many research efforts have been made on crystal growth, electrode preparation and encapsulation of CdZnTe detector, with encouraging achievements [4–8]. However, CdZnTe detector performance is affected by transport characteristics of current carrier generated by incident photons. Although typical electronic mobility of CdZnTe crystal can be 1000 $cm^2\ V^{-1}\ S^{-1}$, the hole mobility is only 100 $cm^2\ V^{-1}\ S^{-1}$ [9–12]. Therefore, holes of slow mobility cannot be collected completely in the short charge collection time, hence the decrease in signal amplitude. This causes serious hole tailing and deteriorates energy resolution, under high counting rates.

To overcome the hole tailing effect, one usually uses single charge carrier readout technique to collect just the electron signal. At present, this can be realized in two ways. One is the electronic methods, including rise-time discrimination [13–15] and bi-parametric analysis [16]. Another is to design appropriate electrode structures, including coplanar electrodes [7], frish grid electrodes [17], pixel electrodes [18] and so on. The electronic method is easier to realize.

In this paper, an analog rise-time discriminator is designed and the discrimination threshold of rise time is set to abandon the signals with incomplete charge collection. Compared to the methods of bi-parametric analysis and digital rise-time discrimination, this method can discriminate original pulse signal directly, and the algorithm is not complex. It overcomes the problem of counting loss caused by inaccurate algorithm, hence better stability. Finally, a portable low power consumption and high-resolution energy spectrometer for CdZnTe detector is designed by combining the discriminator and digital multi-channel analyzer (DMCA).

2 Principle of rise-time discriminator

Incident photons interact with sensitive region of the detector, generating electron–hole pairs. In the external electric field, electron–hole pairs move toward a certain direction and form current pulse signal. The charges collected by the detector, Q, can be related to the current signal output by the detector, $i(t)$, by Eq. (1):

$$Q = \int_{0}^{t_{\mathrm{w}}} i(t)\mathrm{d}t, \tag{1}$$

where t_{w} is charge collection time. When the open-loop gain of preamplifier is large enough, voltage amplitude of charge signal $V_0(t)$ output is Q over the feedback capacitance of the charge-sensitive preamplifier (CSP):

$$V_0(t) \approx Q/C_{\mathrm{f}}. \tag{2}$$

From Eq. (1), when Q is fixed, the higher the $i(t)$, the smaller is the t_{w} and the shorter is the rise time of the charge signal output by CSP. In other words, current signal amplitude is inversely proportional to charge collection time. From Eq. (2), when C_{f} is fixed, $V_0(t)$ is proportional to Q. Therefore, current signal output by the detector can be discriminated through comparing different output charge signals of CSP. Specifically, Eq. (2) shows that the output charge signal of CSP is fixed when incident photons are of the same energy. According to Eq. (1), amplitude of the current signal after being processed by differentiating circuit is determined by rise time of the charge signal. As a result, rise time can be discriminated by time-invariant impulse processing technique through comparison between the delayed current signal and the charge signal. The discrimination threshold of rise time can be adjusted by changing attenuation coefficient of the charge signal [19]. The discrimination process is shown in Fig. 1. Waveforms 1–3 are the ideal total integral charge signal, the reference charge signal and the delayed current signal, respectively; and T_{d} is the delayed time of current signal. Since amplitude of the delayed current signal is higher than that of the reference charge signal, the signal rise time is smaller than the preset time threshold (Fig. 1a, b). At this moment, the detected total integral charge signal represents fast rise-time signal, which will be retained. In Fig. 1c, d, amplitude of the delayed current signal is smaller than that of the reference charge signal and the signal rise time is longer than that of the preset time threshold. The detected total integral charge signal will be abandoned.

3 Design of rise-time discriminator

An analog rise-time discriminator was designed based on the rise-time discrimination principle (Fig. 2). It mainly consists of the differential shaping circuit, charge integrating circuit, deconvolution time-delay circuit, voltage discrimination circuit, comparator circuit and monostable trigger circuit. The differential shaping circuit is to separate DC volume in a signal and converts the bi-exponential signal, which is output by the CSP and has long fall time, into a bi-exponential signal with appropriate fall time via differential shaping. The converted signal accesses to the charge integrating circuit, deconvolution time-delay circuit and voltage discrimination circuit, respectively. The charge integrating circuit is to acquire the reference charge signal. The deconvolution time-delay circuit is to recover bi-exponential signal formed by differential processing into current pulse signal and collect the delayed current signal by using a delayer. The reference charge signal and delayed current signal are compared in a comparator, and results are used to activate the monostable trigger circuit. Meanwhile, voltage discrimination circuit is used in the discriminator to reduce influences of circuit noise. Signals of lower amplitudes than the trigger threshold are eliminated, so as not to have false triggering in the circuit caused by noise. Trigger signal is sent to DMCA by the monostable trigger circuit when output signal rise time of the differential shaping circuit is shorter than the preset threshold, and the circuit noise does not activate the voltage discrimination circuit. The DMCA keeps the amplitude analysis, but it cannot receive trigger signal and corresponding amplitude analysis is abandoned. Implementations of main circuits of the rise-time discriminator will be introduced in the following text.

3.1 Differential shaping circuit

Output signal of the CSP contains DC offset that will disturb rise-time discrimination. A CR differential circuit was designed to isolate such DC offset. It transforms the original pulse signal with long falling edge into bi-exponential signal with narrow pulse width. This not only ensures the signal to well match with the post-integral shaper, but also increases the pulse advancing counting rate. Since the signal after CR differential shaping has posteriori undershoot and undershoot of large signal makes the post-amplifying circuit overloaded, the shaping circuit often adopts parallel connection of an

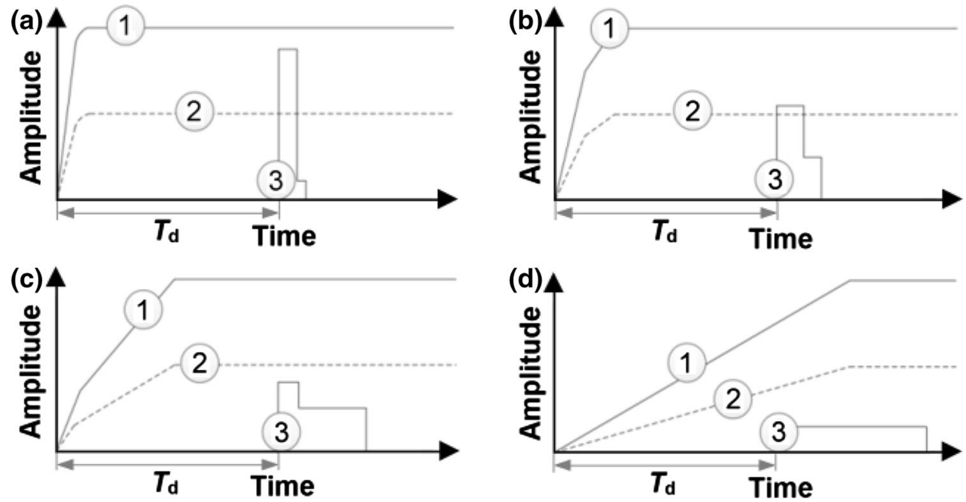

Fig. 1 Principle of rise-time discrimination

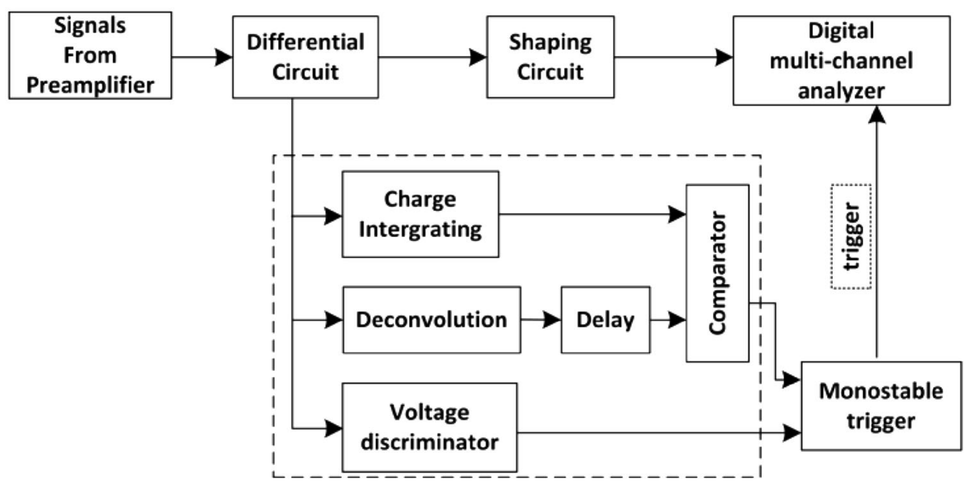

Fig. 2 Block diagram of rise-time discrimination circuit

adjustable potentiometer on the capacitance of the differential circuit. A pole-zero cancellation circuit that could eliminate effect of overshoot was formed. The differential shaping circuit is shown in Fig. 3a. The first-stage differentiating time constant is set as 3 μs. According to $\tau = RC$, if $C10 = 1$ nF, we have $R15 = 3$ kΩ.

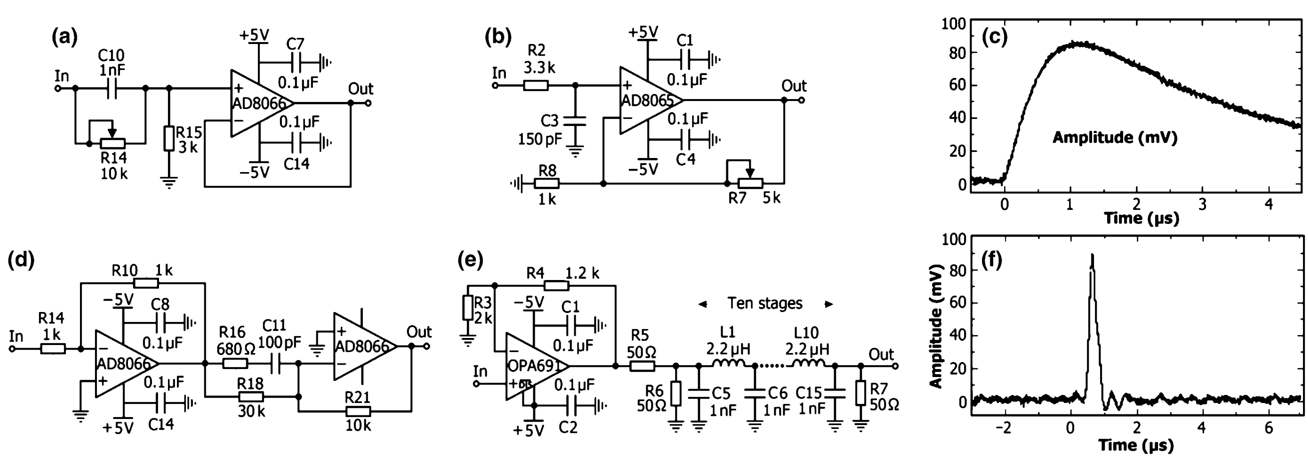

Fig. 3 Differential shaping circuit (**a**), charge integrating circuit (**b**) and its output signal (**c**); and the deconvolution circuit (**d**), LC delay circuit (**e**) and its output signal (**f**)

For circuit stability, the AD8066 operational amplifier, with high speed, low noise, wide bandwidth and high slew rate, is used to form an emitter follower circuit that can enhance current driving capability, achieve matching pre-impedance and post-impedance, isolate reverse disturbances and guarantee circuit stability, without influencing the signal rise time.

3.2 Charge integrating circuit

Amplitude of the CSP output signal is total charges collected by CdZnTe detector in this time period. To get integral output current signal of the CdZnTe detector, the charge collection shall be as complete as possible. This requires a charge integrating circuit with appropriate time constant. The CdZnTe detector is 4 mm × 4 mm × 2 mm (2-mm thick), typical mobilities of electrons (μ_e) is about 1000 cm^2 V^{-1} S^{-1}, and mobilities of holes (μ_h) is about 100 cm^2 V^{-1} S^{-1}. The reverse bias (U_{bias}) applied on the detector circuit is 800 V. The calculation formula of carrier drift velocity is

$$v = \mu E = \mu U_{\mathrm{bias}}/d. \tag{3}$$

Then, the drift velocity of electrons is $v_e = 4 \times 10^6$ cm/s, and the drift velocity of holes is $v_h = 1.3 \times 10^5$ cm/s.

The carrier drift time can be calculated by

$$t = d/v, \tag{4}$$

so, the collection time of electrons is $t_e = 50$ ns and the collection time of holes is $t_h = 500$ ns.

Therefore, time constant (τ) of the integral circuit can be set as 500 ns. In the actual circuit (Fig. 3b), $R2$ is 3.3 kΩ and $C3$ is 150 pF. To make discrimination threshold of rise time adjustable, a charge comparison signal output circuit with gain control was designed based on the AD8065 operational amplifier. Amplitude of the charge comparison signal can be adjusted by controlling the potentiometer $R7$.

3.3 Deconvolution time-delay circuit [20]

Since signal output by the CdZnTe detector can be viewed as an ideal δ function, and the signal being processed by the CSP and differential shaping circuit to input into the post-discriminator is exponential, the CSP and differential shaping circuit can be regarded as a convolution operation circuit. The system response is shown in Fig. 4. A1 and A2 are ideal amplifier. The current pulse signal output by the CdZnTe detector is converted into a standard voltage signal by the ideal current–voltage converter. Later, a bi-exponential pulse signal is acquired after RC low-pass network processing.

The post-comparison circuit needs current pulse signal, so the bi-exponential signal has to be restored into the current pulse signal through deconvolution. Since the output voltage signal and the input current signal of the current–voltage converter have the same shape, the signal that has been convoluted by detector–amplifier–differentiator can be deconvoluted by searching the inverse transfer function of RC low-pass network. A pulse response linear time-invariant system of δ function is gained from convolution of a signal and low-pass filter. The deconvolution pulse response of this system can be acquired from the deconvolution transfer function by transforming the low-pass filter impulse response into the δ function.

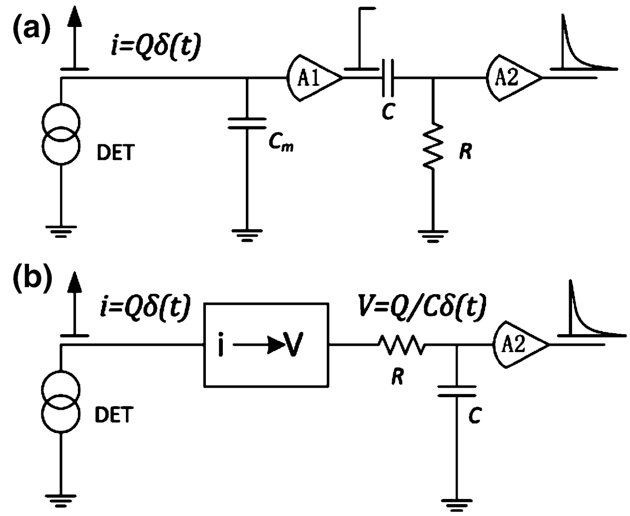

Fig. 4 Ideal amplifier for detector

According to Ref. [21], impulse response of RC low-pass filter is

$$h(t) + \tau\frac{\mathrm{d}h(t)}{\mathrm{d}t} = \delta(t), \quad (t > 0, h(0) = 0). \tag{5}$$

Therefore, the output signal (V_{out}) can be related to the input signal (V_{in}) of the low-pass filter by Eq. (6),

$$v_{\mathrm{out}}(t) = v_{\mathrm{in}}(t) + \tau dv_{\mathrm{in}}(t)/\mathrm{d}t. \tag{6}$$

So, the impulse response of deconvolution is

$$h'(t) = \delta(t) + \tau\delta(t). \tag{7}$$

From Eqs. (5) and (6), the convolution of $h'(t)$ and $h(t)$ is

$$-h(t) * h'(t) = \delta(t). \tag{8}$$

On this basis, the deconvolution circuit is designed (Fig. 3d), in which the time constant shall be in accordance with that of exponential signal of preceding stage. To avoid over high breakover current caused by small capacitive reactance, a current-limiting resistance $R16$ is added into the capacitance. Also, the value of $R16$ multiplied by $C11$ must be far smaller than the value of $R18$ multiplied by $C11$ to prevent significant influence of $R16$ on time constant of this deconvolution circuit.

It takes 500 ns for the charge integrating circuit to process the original signal and get the reference charge signal. To ensure the current signal gained by the deconvolution circuit comparable with the peak of reference charge signal at the same time, current signal shall be delayed to a certain extent. A LC delay circuit was designed (Fig. 3e). The total delay time shall be consistent with the charge integrating time. The OPA691 current feedback operational amplifier is used as the driver chip, because the LC delay circuit needs certain drive currents, especially when there are many delay grades and the current provided by front deconvolution circuit is inadequate to maintain normal operation of the delay circuit. To safeguard normal signal transformation, 50 Ω resistances have to be added between its input and ground and between its output and ground to safeguard normal signal transformation.

For an LC delay circuit, the delay time is $T = (LC)^{1/2}$, and equivalent impedance is $Z = (L/C)^{1/2}$, so we have

$$L = nL_n = TZ, \tag{9}$$

where n is stage number. Since the number of stage of an actual delayed circuit is limited and every stage can be viewed as a low-pass filter, the cutoff frequency is

$$\omega_C = (L_n C_n)^{-1/2} = n/T. \tag{10}$$

The existence of cutoff frequency will cause delay line dispersion. The pulse rise time and fall time are

$$\tau = 1/\omega_C = T/n. \tag{11}$$

In this design, $T = 500$ ns, $Z = 50\ \Omega$ and $\tau = 50$ ns. According to Eqs. (9–11), we have $n = 10$, $L_n = 2.5$ H and $C_n = 1$ nF.

The actual circuit can realize signal delay by using a 10-stage LC circuit, with the inductance of 2.2 μH and capacitance of 1 nF for each delay circuit. The actual delayed time of each stage is 46.9 ns. Considering signal delay by deconvolution circuit and current drive circuit, the total delayed time of the deconvolution circuit is about 500 ns.

3.4 Voltage discriminator and monostable trigger circuit

Influenced by noises, the charge integrating access and the deconvolution delay access will generate false trigger signals. It is necessary to set a threshold of effective signal through voltage discriminator and gate circuit to extract effective trigger pulse. This design uses the ultra-fast comparator TL3016 as the voltage discriminator. Threshold voltage is set as 20 mV by a resistor divider at the inverting input terminal, and the original signal is accessed into the non-inverting input. The comparator can output high level when input signal is bigger than circuit noise. The other comparator is connected with the delayed current signal at the non-inverting input terminal and the reference charge signal at the inverting input terminal. It only can output high level when the delayed current signal is bigger than the reference charge signal. The rise time is higher than the discriminator threshold. Finally, effective trigger pulse can be gained by making output signals of two comparators passing through the AND gate. The trigger pulse is narrow when there is a small difference between the current signal and the charge signal, which goes against the DMCA reception. Therefore, a monostable trigger circuit has to be designed to ensure that the signal has an appropriate high-level retention time.

4 Performance test

4.1 Rise-time discriminator test

Threshold of the rise-time discrimination circuit determines performance of the whole discriminator. Since rise

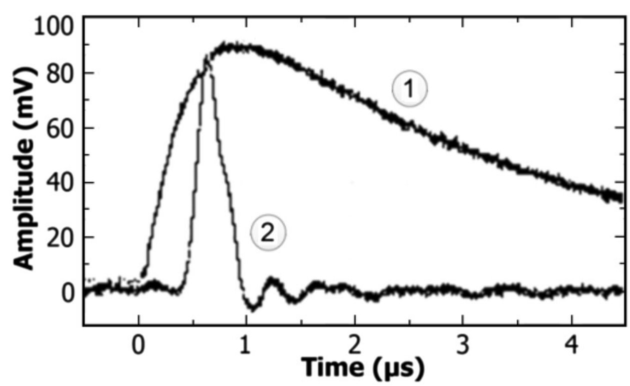

Fig. 5 Comparison of delayed current signal and reference charge signal

Table 1 Whether trigger in differential rise time

Rise time (ns)	V_{Ref} (mV)	V_{Delay} (mV)	Trigger?
100	88	132	Yes
150	88	116	Yes
200	88	112	Yes
250	88	97	Yes
300	88	88	Indefinite
350	80	68	No
400	72	52	No
450	66	46	No
500	60	40	No
550	58	36	No
600	56	32	No

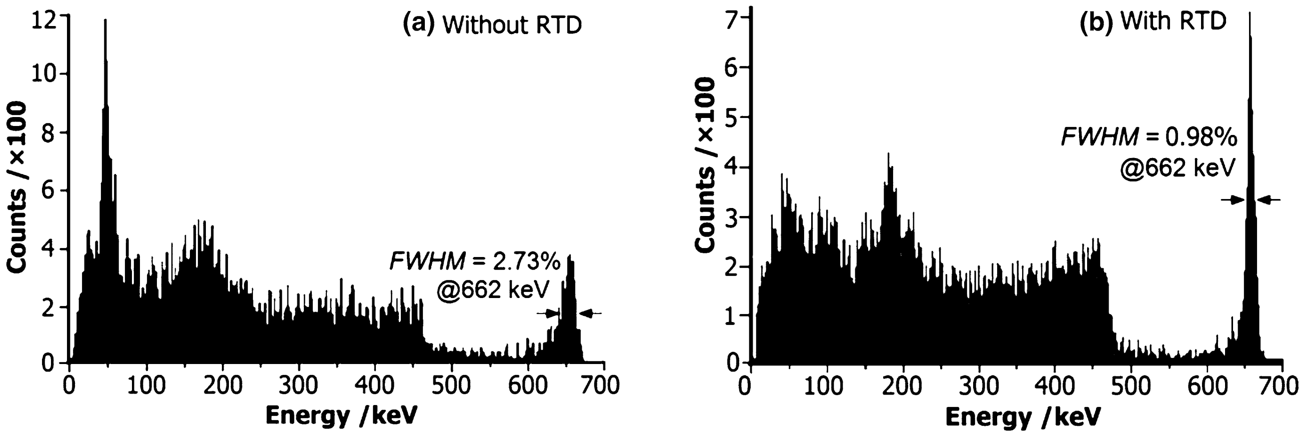

Fig. 6 Spectra of ^{137}Cs without and with rise-time discrimination

time of an effective signal in CdZnTe detector is about 200 ns, the discriminator threshold is designed at 300 ns to retain effective signals. The discriminator threshold is determined by the reference charge signal amplitude after the delayed current signal is determined. A bi-exponential signal with 300 ns rising edge is input. Next, amplitude of the reference charge signal is adjusted equal to that of the delayed current signal at the same time. As shown in Fig. 5, Curve 1 is the reference charge signal and Curve 2 is the delayed current signal. If the rise-time threshold is 300 ns, parameters of the discrimination circuit can be determined.

To verify validity of parameters, rise time of the bi-exponential signal is adjusted from 100 to 600 ns in 50-ns steps. To make sure that the bi-exponential signal and the output signal of preamplifier have equal amplitude, input signal amplitude of the discrimination circuit is set at 35 mV. Delayed current signal and reference charge signal are listed in Table 1.

From Table 1, when rise time of the original current signal is below 300 ns, a trigger pulse is produced; at 300 ns, it is uncertain whether trigger pulse can be produced because of noises; when the rise time is over 300 ns, the discrimination circuit cannot be triggered. This reflects that the designed rise-time discrimination circuit can trigger effective signals in the CdZnTe detector.

4.2 Energy spectrum measurement

Figure 6 is the energy spectrum of ^{137}Cs source without and with rise-time discriminator, measured by a 4 mm × 4 mm × 2 mm CdZnTe detector provided by Northwestern Polytechnical University. Without the rise-time discriminator, the tailing effect is obvious in the 662 keV peak, with an energy resolution of just 2.73%, due to the changing rise time or incomplete charge collection. With the rise-time discriminator at the threshold of 300 ns, the tailing effect of the 662 keV peak is improved significantly and the energy resolution reaches as high as 0.98%.

5 Conclusion

To solve the hole tailing effect caused by incomplete charge collection in CdZnTe detector, an analog rise-time discriminator was designed, which could recognize the rise time of signals output by CSP and eliminate signals with rise time higher than the threshold. It overcomes the problem of worse energy resolution in traditional energy spectrometer caused by variation of charge collection time. This rise-time discriminator has adjustable rise-time threshold, low power consumption, simple structure and high improvement of system energy resolution and is applicable to portable high-resolution energy spectrometer.

References

1. J. Franc, P. Höschl, E. Belas et al., CdTe and CdZnTe crystals for room temperature gamma-ray detectors. Nucl. Instrum. Methods Phys. Res. A. **434**, 146–151 (1999). doi:10.1016/S0168-9002(99)00448-9
2. T.E. Schlesinger, J.E. Toney, H. Yoon et al., Cadmium zinc telluride and its use as a nuclear radiation detector material. Polym. Mater. Sci. Eng. **32**, 103–189 (2001). doi:10.1016/S0927-796X(01)00027-4
3. L. Abbene, S. Del Sordo, F. Fauci et al., Spectroscopic response of a CdZnTe multiple electrode detector. Nucl. Instrum. Methods Phys. Res. A. **583**, 324–331 (2007). doi:10.1016/j.nima.2007.09.015
4. G. Yang, A.E. Bolotnikov, P.M. Fochuk et al., Post-growth thermal annealing study of CdZnTe for developing room-temperature X-ray and gamma-ray detectors. J. Cryst. Growth **379**, 16–20 (2013). doi:10.1016/j.jcrysgro.2012.11.041
5. H. Yücel, E. Uyar, A.N. Esen, Measurements on the spectroscopic performance of CdZnTe coplanar grid detectors. Appl.

Radiat. Isot. **70**, 1608–1615 (2012). doi:10.1016/j.apradiso.2012.04.027
6. P.N. Luke, Single-polarity charge sensing in ionization detectors using coplanar electrodes. Appl. Phys. Lett. **65**, 2884–2886 (1994). doi:10.1063/1.112523
7. P.N. Luke, Unipolar charge sensing with coplanar electrodes-application to semiconductor detectors. IEEE Trans. Nucl. Sci. **42**, 207–213 (1995). doi:10.1109/23.467848
8. Z. He, Potential distribution within semiconductor detectors using coplanar electrodes. Nucl. Instrum. Methods Phys. Res. A. **365**, 572–575 (1995). doi:10.1016/0168-9002(95)00676-1
9. C. Szeles, Advances in the crystal growth and device fabrication technology of CdZnTe room temperature radiation detectors. IEEE Trans. Nucl. Sci. **51**, 1242–1249 (2004). doi:10.1109/TNS.2004.829391
10. H. Chen, S. Awadalla, K. Iniewski et al., Characterization of large cadmium zinc telluride crystals grown by traveling heater method. Appl. Phys. **103**, 014903 (2008). doi:10.1063/1.2828170
11. A. Shor, Y. Eisen, Israel Mardor, Spectroscopy with CdZnTe γ- and X-ray detectors by modifying the electron trapping to compensate for incomplete charge collection caused by large hole trapping. Nucl. Instrum. Methods Phys. Res. A. **426**, 491–496 (1999). doi:10.1016/S0168-9002(99)00023-6
12. G.F. Knoll, *Radiation Detection and Measurement*, 3rd edn. (Wiley, New York, 2000), pp. 353–357
13. J. Töke, M.J. Quinlan, W. Gawlikowicz et al., A simple method for rise-time discrimination of slow pulses from charge-sensitive preamplifiers. Nucl. Instrum. Methods Phys. Res. A. **595**, 460–463 (2008). doi:10.1016/j.nima.2008.07.024
14. V. Esmaeili-sani, A. Moussavi-zarandi, N. Akbar-ashrafi et al., Neutron–gamma discrimination based on bipolar trapezoidal pulse shaping using FPGAs in NE213. Nucl. Instrum. Methods Phys. Res. A. **694**, 113–118 (2012). doi:10.1016/j.nima.2012.08.025
15. C. Imperiale, A. Imperiale, On nuclear spectrometry pulses digital shaping and processing. Measurement **30**, 49–73 (2001). doi:10.1016/S0263-2241(00)00057-9
16. N. Auricchio, L. Amati, A. Basili et al., Twin shaping filter techniques to compensate the signals from CZT/CdTe detectors. IEEE Trans. Nucl. Sci. **52**, 1982–1988 (2005). doi:10.1109/TNS.2005.856884
17. D.S. McGregor, Z. He, H.A. Seifert et al., Single charge carrier type sensing with a parallel strip pseudo-Frisch-grid CdZnTe semiconductor radiation detector. Appl. Phys. Lett. **72**, 792–794 (1998). doi:10.1063/1.120895
18. M. Mayer, L.A. Hamel, O. Tousignant et al., Signal formation in a CdZnTe imaging detector with coplanar pixel and control electrodes. Nucl. Instrum. Methods Phys. Res. A. **422**, 190–194 (1999). doi:10.1016/S0168-9002(98)01126-7
19. A. Niemelä, H. Sipilä, V.I. Ivanov, Improving CdZnTe X-ray detector performance by cooling and rise time discrimination. Nucl. Instrum. Methods Phys. Res. A. **377**, 484–486 (1996). doi:10.1016/0168-9002(96)00028-9
20. V.T. Jordanov, Deconvolution of pulses from a detector-amplifier configuration. Nucl. Instrum. Methods Phys. Res., Sect. A **351**, 592–594 (1994). doi:10.1016/0168-9002(94)91394-3
21. A.V. Oppenheim, A.S. Willsky, *Signals and Systems* (Tsinghua University Press, Beijing, 1999), p. 74